Kren A, Baeriswyl V, Lehembre F et al.Increased tumor cell dissemination and cellular senescence in the absence of beta1-integrin function. EMBO J 26:2832-2842

ARTICLE *in* THE EMBO JOURNAL · JULY 2007

Impact Factor: 10.43 · DOI: 10.1038/sj.emboj.7601738 · Source: PubMed

The EMBO Journal (2007) 26, 2832–2842 | © 2007 European Molecular Biology Organization | All Rights Reserved 0261-4189/07
www.embojournal.org

THE EMBO JOURNAL

Increased tumor cell dissemination and cellular senescence in the absence of β_1-integrin function

Angelika Kren[1], Vanessa Baeriswyl[1], François Lehembre[1], Christoph Wunderlin[1], Karin Strittmatter[1], Helena Antoniadis[1], Reinhard Fässler[2], Ugo Cavallaro[3] and Gerhard Christofori[1,*]

[1]Institute of Biochemistry and Genetics, Department of Clinical-Biological Sciences, Center of Biomedicine, University of Basel, Switzerland, [2]Max-Planck-Institute of Biochemistry, Department of Molecular Medicine, Martinsried, Germany and [3]IFOM-FIRC Institute of Molecular Oncology, Milano, Italy

Integrins are transmembrane receptors that bind extracellular matrix proteins and enable cell adhesion and cytoskeletal organization, as well as transduction of signals into cells, to promote various aspects of cellular behavior, such as proliferation or survival. Integrins participate in many aspects of tumor biology. Here, we have employed the Rip1Tag2 transgenic mouse model of pancreatic β cell carcinogenesis to investigate the role of β_1-integrin in tumor progression. Specific ablation of β_1-integrin function in pancreatic β cells resulted in a defect in sorting between insulin-expressing β cells and glucagon-expressing α cells in islets of Langerhans. Ablation of β_1-integrin in β tumor cells of Rip1Tag2 mice led to the dissemination of tumor cell emboli into lymphatic blood vessels in the absence of ongoing lymphangiogenesis. Yet, disseminating β_1-integrin-deficient β tumor cells did not elicit metastasis. Rather, primary tumor growth was significantly impaired by reduced tumor cell proliferation and the acquisition of cellular senescence by β_1-integrin-deficient β tumor cells. The results indicate a critical role of β_1-integrin function in mediating metastatic dissemination and preventing tumor cell senescence.

The EMBO Journal (2007) **26,** 2832–2842. doi:10.1038/sj.emboj.7601738; Published online 31 May 2007
Subject Categories: cell & tissue architecture; molecular biology of disease
Keywords: cell adhesion; β_1-integrin; metastasis; senescence; tumorigenesis

Introduction

The integrin family of transmembrane receptors consists of eight β and 18 α subunits that assemble as heterodimers to form 24 distinct integrins (Hynes, 2002). The main ligands for integrins in the extracellular space are extracellular matrix proteins, such as laminin and collagen, as well as cellular counter-receptors. On their cytoplasmic domains, integrins are linked to the cytoskeleton, which they regulate and modulate via various sub-membrane linker proteins (Zamir and Geiger, 2001). Integrins transduce signals across the plasma membrane in both directions: integrin binding to its ligands requires its activation by inside-out signals. Conversely, integrin ligation triggers outside-in signals that regulate different aspects of cell behavior, including cell survival, control of transcription, cell proliferation, cell motility and cytoskeletal organization (Hynes, 2002).

Due to their broad spectrum of features, integrins and integrin signaling have been shown to contribute to tumor progression in various ways (Guo and Giancotti, 2004). For example, recent reports have highlighted the role of β_4-integrin in promoting mammary tumor progression by amplifying ErbB2 signaling and thereby activating the transcription factors STAT3 and c-Jun (Guo *et al*, 2006). On the other hand, $\alpha_v\beta_3$, $\alpha_v\beta_5$ and several integrins of the β_1 class have been implicated in angiogenesis. Indeed, inhibition of these molecules by antagonist molecules or specific antibodies against integrins efficiently blocks angiogenesis (Brooks *et al*, 1994, 1995; Friedlander *et al*, 1995; Sudhakar *et al*, 2003). Excessive joint signaling by β_1-integrin and tyrosine kinase receptors has been associated with disruption of adherens junctions, a prerequisite for metastatic invasion of cancer cells (Novak *et al*, 1998; Tan *et al*, 2001; Fujita *et al*, 2002; Zhang *et al*, 2003). Cell type-specific ablation of β_1-integrin function in the mouse has demonstrated that this integrin plays a key role in regulating cell cycle progression of luminal mammary epithelial cells and is critical for the alveolar morphogenesis of glandular epithelium (Li *et al*, 2005; Naylor *et al*, 2005). Furthermore, β_1-integrin expression has been proven critical for the initiation of mammary tumorigenesis *in vivo*, and for maintaining the proliferative capacity of late-stage tumor cells (White *et al*, 2004).

We have set out to investigate the functional role of β_1-integrin during tumor progression in Rip1Tag2 transgenic mice. In Rip1Tag2 mice (RT2 mice), the Simian Virus 40 large T antigen is expressed under the control of the rat insulin promoter, resulting in the reproducible development of pancreatic β cell tumors (insulinomas) following a highly reproducible multistage tumorigenesis pathway (Hanahan, 1985). Our laboratories have previously reported that RT2 mice that are deficient for the expression of neural cell adhesion molecule (NCAM), RT2;NCAM$^{-/-}$ mice, show striking disintegration of the tumor tissue architecture, and together with upregulated lymphangiogenesis, develop metastases to the local draining lymph nodes of the pancreas (Perl *et al*, 1999). Subsequent biochemical analyses have revealed that, by binding to and stimulating fibroblast growth factor (FGF) receptors, NCAM activates signaling pathways leading to the activation of β_1-integrin-mediated cell–matrix adhesion (Cavallaro *et al*, 2001). Based on such epistatic relation between NCAM and β_1-integrin functions, and the fact that the loss of NCAM function leads to lymph node metastasis in

*Corresponding author. Institute of Biochemistry and Genetics, Department of Clinical Biological Sciences, Center of Biomedicine, University of Basel, Mattenstrasse 28, Basel 4058, Switzerland.
Tel.: +41 61 267 3564; Fax: +41 61 267 3566;
E-mail: Gerhard.Christofori@unibas.ch

Received: 24 December 2006; accepted: 8 May 2007; published online: 31 May 2007

Rip1Tag2 mice, we hypothesized that the loss of β_1-integrin may at least in part recapitulate the loss of NCAM function.

We report here that deletion of β_1-integrin function during the development of islets of Langerhans results in a defect of the sorting of endocrine α and β cells in islets. Ablation of β_1-integrin expression during β cell tumorigenesis in Rip1Tag2 mice led to the dissemination of tumor cell emboli into lymphatic vessels but did not induce increased lymphangiogenesis or metastasis. Mice carrying β_1-integrin-deficient tumors exhibited reduced tumor burden, reduced tumor cell proliferation and the induction of cellular senescence, potentially via a pathway involving the upregulation of the cell-dependent kinase inhibitor $p21^{Cip1}$. Consistent with these results, tumor cells that lack β_1-integrin were not able to form tumors or metastases in tumor transplantation experiments. Together, the results highlight a critical role of β_1-integrin in the metastatic dissemination of tumor cells and in cellular senescence.

Results

β_1-integrin is required for islet cell sorting

Complete loss of β_1-integrin function in β_1-integrin knockout mice results in embryonic lethality (Fassler and Meyer, 1995). We therefore employed mice carrying β_1-integrin alleles flanked by loxP sites ($\beta1^{(fl/fl)}$ mice) (Potocnik *et al*, 2000) to ablate β_1-integrin function specifically in normal pancreatic β cells and β tumor cells, by crossing them to mice expressing the Cre recombinase under the control of the β cell-specific rat insulin promoter (RCre) (Ahlgren *et al*, 1998), and subsequently with Rip1Tag2 mice.

To assess the effects of β_1-integrin deletion during normal islet development, islets of RCre;$\beta1^{(fl/fl)}$ mice were compared to either wild-type C57Bl/6 or $\beta1^{(fl/fl)}$ control mice. Since Cre recombinase is already expressed during islet development in RCre mice, β_1-integrin expression is ablated in insulin-expressing cells at early stages of islet development (Ahlgren *et al*, 1998; Tan *et al*, 2001). Histopathological analysis of 8- to 10-week-old RCre;$\beta1^{(fl/fl)}$ mice showed no apparent changes in islet number, size and architecture (Figure 1A, upper panel and data not shown). However, immunofluorescence stainings of histological sections for insulin and glucagon revealed differences in the organization of islet cells (Figure 1A, lower panel). In control animals, most islets of Langerhans (82.4%) displayed glucagon-producing α cells located within the three most peripheral cell layers of the islets, whereas insulin-expressing β cells were mainly localized in the center of the islets (Figure 1A, lower left panel). Only in a small percentage of control islets α cells were also found within the center of islets (Table I, 17.6%), hereafter referred to as mixed sorting phenotype. In contrast, most islets of RCre;$\beta1^{(fl/fl)}$ mice were of the mixed sorting phenotype (81% mixed versus 19% normal phenotype, Figure 1A, lower right panel and Table I). Average numbers of α cells per islet area were found to be increased in RCre;$\beta1^{(fl/fl)}$ islets as compared with wild-type controls (1.307 α cells/1000 μm^2 versus 2.205 α cells/1000 μm^2; Table I, $P<0.005$, unpaired *t*-test). Together, these results indicate that deletion of β_1-integrin in pancreatic β cells leads to disturbances in cell type segregation during islet development, a phenotype also observed in islets lacking NCAM expression (Esni *et al*, 1999) or expressing a dominant-negative version of E-cadherin in β cells (Dahl *et al*, 1996).

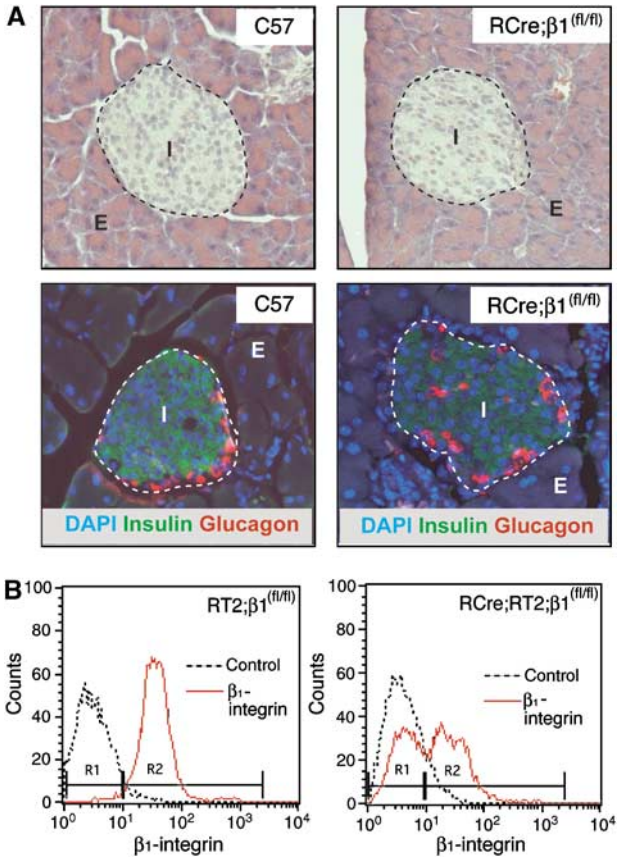

Figure 1 Distorted sorting of α and β cells in β_1-integrin-deficient islets of Langerhans. (**A**) Upper panel: immunohistochemical analysis by hematoxylin and eosin staining of histological sections of pancreatic islets from wild-type (C57) and β_1-integrin-deficient (RCre;$\beta1^{(fl/fl)}$) mice. Lower panel: immunofluorescence co-stainings for insulin (green), glucagon (red) and nuclei (DAPI, blue) of histological sections from wild-type (C57) and β_1-integrin-deficient (RCre;$\beta1^{(fl/fl)}$) mice. (**B**) FACS analysis of tumor cell suspensions from RT2;$\beta1^{(fl/fl)}$ control (left panel) and RCre;RT2;$\beta1^{(fl/fl)}$ experimental (right panel) mice stained for β_1-integrin. Dashed black lines represent unstained cells, solid red line represents cells stained for β_1-integrin.

Table I An endocrine cell sorting phenotype in β_1-integrin-deficient islets

	C57/$\beta_1^{(fl/fl)}$	RCre;$\beta_1^{(fl/fl)}$
n[a]	28	28
% Normal[b]	82.4	19.0
% Mixed[c]	17.6	81.0
α cells per 1000 μm^2[d]	1.307 ± 0.646	2.205 ± 1.122

[a]Number of islets analyzed.
[b]Percentage of islets with glucagon cells in the three outermost cell layers.
[c]Percentage of islets with glucagon cells in the islet center.
[d]$P<0.005$, unpaired *t*-test.

Loss of β_1-integrin induces tumor cell dissemination into lymphatics

To investigate the role of β_1-integrin *in vivo* during Rip1Tag2 tumorigenesis, Rip1Tag2 (RT2) mice were crossed with $\beta1^{(fl/fl)}$ and RCre mice. Recombination of the β_1-integrin gene in

RCre;RT2;$\beta1^{(fl/fl)}$ experimental and RT2;$\beta1^{(fl/fl)}$ control mice was monitored by determining β_1-integrin protein levels in tumors of 12-week-old mice. Dispersed tumor cells were subjected to FACS analysis by performing a CD31 (endothelial cell marker) and β_1-integrin co-staining, excluding endothelial cells from the analysis. More than 95% (96.42 ± 2.34%) of the cells derived from RT2;$\beta1^{(fl/fl)}$ tumors show β_1-integrin expression (region R2 in Figure 1B), whereas in RCre;RT2;$\beta1^{(fl/fl)}$ tumors a second, β_1-integrin negative population appeared (region R1 in Figure 1B). This population represents around 40% (39.24 ± 3.07%) of all analyzed cells. Thus, the $\beta1^{(fl/fl)}$ allele is completely recombined in about 40% of all tumor cells. The ratio between α and β cells was unchanged between tumors of RT2;$\beta1^{(fl/fl)}$ and RCre;RT2;$\beta1^{(fl/fl)}$ mice; in all tumors the majority of cells were insulin-producing β tumor cells (Supplementary Figure 2E).

We have previously reported that β cell tumors in NCAM-deficient mice show increased tumor-associated lymphangiogenesis (Crnic *et al*, 2004), as well as tumor tissue disintegration and increased metastasis (Perl *et al*, 1999). Based on the fact that NCAM modulates β_1-integrin function by stimulating FGF receptor signaling in β tumor cells (Cavallaro *et al*, 2001), we analyzed sections of 11- to 13-week-old RCre;RT2;$\beta1^{(fl/fl)}$ mice for the presence of lymphatic vessels by immunohistochemical staining of pancreatic sections with antibodies against the lymphatic marker LYVE-1 (Banerji *et al*, 1999). Tumors were divided into five groups according to the degree of lymphatic vessels surrounding the tumor perimeter (no lymphatic vessels = 0%, 1–10%, 10–25%, 25–50% or >50% of tumor perimeter covered by lymphatic vessels; Figure 2A). No significant changes in tumor-associated lymphangiogenesis were observed for any defined group. Moreover, as determined by immunohistochemical staining, expression of the lymphangiogenic factors VEGF-C and VEGF-D was not induced in β_1-integrin-deleted tumors (data not shown). From these results, we conclude that the loss of β_1-integrin function does not induce lymphangiogenesis. Moreover, no changes in blood vessel density, morphology, pericyte coverage and tumor-infiltrating inflammatory cells was observed between tumors of RT2;$\beta1^{(fl/fl)}$ and RCre;RT2;$\beta1^{(fl/fl)}$ mice (Supplementary Figure 2A–D).

Ablation of NCAM in the Rip1Tag2 model leads to a severe change in tumor architecture, namely marked tissue disintegration and the appearance of hemorrhagic lacunae (Cavallaro *et al*, 2001; Xian *et al*, 2006). Histological analysis of pancreatic sections from RT2;$\beta1^{(fl/fl)}$ and RCre;RT2;$\beta1^{(fl/fl)}$ tumors did not reveal alterations in the appearance of hemorrhagic lacunae and tissue disintegration between the two different genotype tumors. However, in these experiments and also during the analysis of sections stained for LYVE-1 (see above), we found a significant increase in the number of disseminated tumor cell emboli within lymphatic vessels in the close vicinity of β_1-integrin-deficient tumors (Figure 2B, left panel) or tumor edges (Figure 2B, right panel). Such tumor cell emboli were detected in 60% of all analyzed RCre;RT2;$\beta1^{(fl/fl)}$ mice and only in 7.7% of control mice (Figure 2C). However, detailed macroscopic and microscopic analyses did not reveal the occurrence of metastases in any of the mice, neither to local lymph nodes nor to distant organs. These results suggest that the loss of β_1-integrin, while facilitating the displacement of tumor cell emboli into the lymphatic vasculature, is not sufficient to induce metastasis formation.

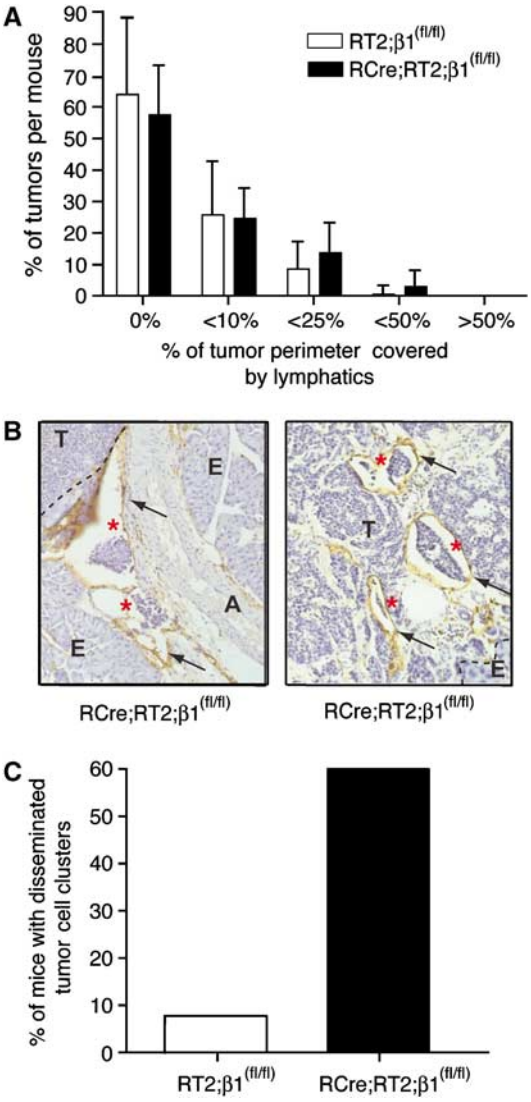

Figure 2 Dissemination of tumor cell emboli but no lymphangiogenesis in β_1-integrin-deficient tumors of RT2 mice. (**A**) Determination of peritumoral lymphatic density. White bars, tumors of RT2;$\beta1^{(fl/fl)}$ mice (12 mice, 162 tumors); black bars, tumors of RCre;RT2;$\beta1^{(fl/fl)}$ mice (15 mice, 205 tumors). Tumor sections were stained for LYVE-1 and categorized according to the degree of lymphatic coverage: not in contact with any lymphatic vessel (0%), tumors that were surrounded less than 10% (<10%), less than 25% (<25%), less than 50% (<50%) and more than 50% of (>50%). Statistical analysis (unpaired *t*-test) indicated that differences within groups are not significant. (**B**) LYVE-1 staining (brown, indicated by arrows) of histological sections of pancreata from RCre;RT2;$\beta1^{(fl/fl)}$ mice. Circulating tumor cell clusters are indicated by red asterisks. A, artery; E, exocrine pancreas; T, tumor. (**C**) Percentage of mice showing disseminated tumor cell clusters in RT2;$\beta1^{(fl/fl)}$ (white bars, $n = 12$) and RCre;RT2;$\beta1^{(fl/fl)}$ mice (black bars; $n = 15$).

Loss of β_1-integrin-mediated cell–matrix adhesion

To investigate how the deletion of β_1-integrin contributes to the dissemination of tumor cells, we established cell lines from RCre;RT2;$\beta1^{(fl/fl)}$ experimental as well as RT2;$\beta1^{(fl/fl)}$ control tumors. PCR analysis confirmed the presence of two floxed β_1-integrin alleles in control cells ($\beta Ti^{(fl/fl)}$), and of two deleted alleles in cells derived from experimental tumors ($\beta Ti^{(\Delta/\Delta)}$; Figure 3A, upper panel). Cell lines derived from tumors of normal Rip1Tag2 mice (βT2) and of NCAM-

deficient Rip1Tag2 mice (βTN2; Cavallaro *et al*, 2001), both carrying wild-type β_1-integrin alleles, were employed as controls (Figure 3A, upper panel). FACS analysis revealed that $\beta Ti^{(fl/fl)}$, βT2 and βTN2 expressed comparable levels of β_1-integrin at their cell surface (data not shown) and confirmed that $\beta Ti^{(\Delta/\Delta)}$ cells indeed had lost β_1-integrin expression (Figure 3B). When establishing primary tumor cell lines from tumors of Rip1Tag2 mice, some cell lines still express high levels of NCAM, whereas others do not. Since both $\beta Ti^{(fl/fl)}$ cells and β_1-integrin-deficient $\beta Ti^{(\Delta/\Delta)}$ cell lines expressed only low amounts of NCAM, the βT2 cell line that expressed high levels of NCAM and the βTN2 cell line that did not express any NCAM were included to directly compare the function of NCAM and β_1-integrin in β tumor cells side by side (Figure 3A, lower panel).

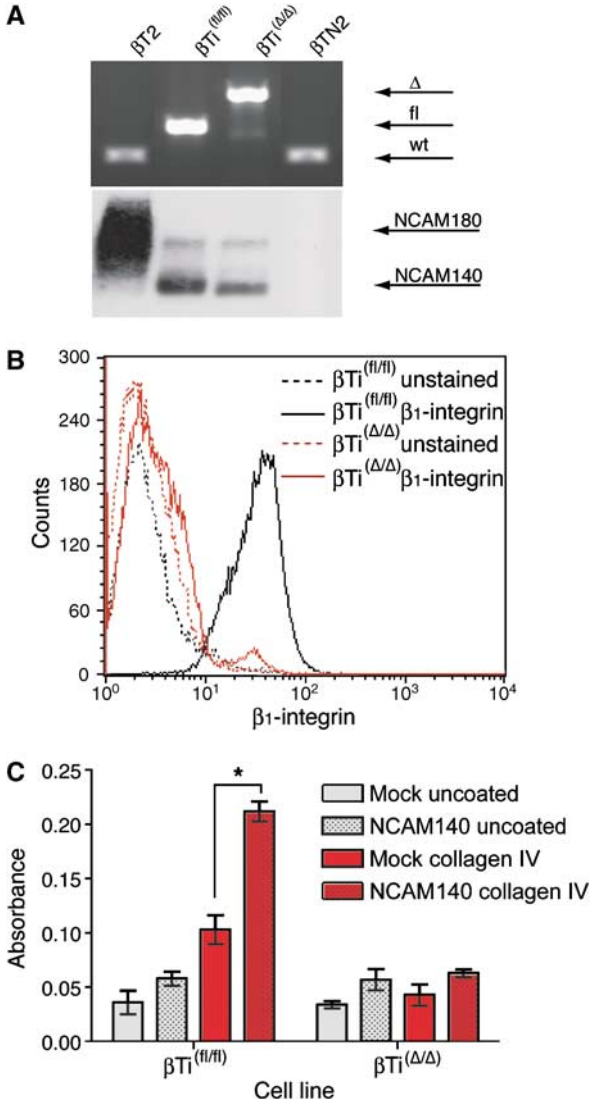

Figure 3 Cell lines derived from RT2;$\beta1^{(fl/fl)}$ and RCre;RT2;$\beta1^{(fl/fl)}$ tumors. (**A**) Top panel: genotyping of cell lines derived from RT2 (βT2), RT2;$\beta1^{(fl/fl)}$ ($\beta Ti^{(fl/fl)}$), RCre;RT2;$\beta1^{(fl/fl)}$ ($\beta Ti^{(\Delta/\Delta)}$), and RT2;$NCAM^{-/-}$ (βTN2) tumors by PCR analysis. wt, wild-type β_1-integrin alleles; fl, floxed alleles; Δ, deleted alleles. Bottom panel: immunoblotting analysis of NCAM expression in βT2, $\beta Ti^{(fl/fl)}$, $\beta Ti^{(\Delta/\Delta)}$ and βTN2 cells. (**B**) FACS analysis of β_1-integrin surface expression levels of $\beta Ti^{(fl/fl)}$ (black line) and $\beta Ti^{(\Delta/\Delta)}$ (red line). Dashed lines represent controls (unstained cells). (**C**) Adhesion of the different genotype β tumor cells to collagen IV. Mock-transfected (clear bars) or NCAM140-transfected (dotted bars) $\beta Ti^{(fl/fl)}$ and $\beta Ti^{(\Delta/\Delta)}$ β tumor cell lines were seeded on either uncoated (gray bars) or collagen IV-coated (red bars) culture dishes. $^*P<0.003$, unpaired *t*-test.

Previously, we have reported that the activation of β_1-integrin-mediated adhesion of β tumor cells to collagen type IV is abrogated in NCAM-deficient βTN2 cells and can be re-established by re-introducing NCAM (Cavallaro *et al*, 2001). We thus compared the adhesion capabilities of $\beta Ti^{(fl/fl)}$ and $\beta Ti^{(\Delta/\Delta)}$ cell lines in the presence or absence of NCAM. Equal amounts of cells were seeded on plates coated with various matrix proteins, and adhering cells were scored (Figure 3C). Adhesion of the $\beta Ti^{(\Delta/\Delta)}$ cell line to collagen IV was very low and could not be increased by forced expression of NCAM140. Adhesion of Mock-transfected $\beta Ti^{(fl/fl)}$ cells was comparable to that of $\beta Ti^{(\Delta/\Delta)}$ cells, however, forced expression of NCAM140 significantly stimulated adhesion to collagen IV ($P<0.05$, unpaired *t*-test) but not to collagen type I, fibronectin or uncoated plastic (Table III). Cultured β tumor cells are known to lack significant migratory and invasive capabilities (Cavallaro *et al* 2001), and this feature was not changed by the loss of β_1-integrin function. These results further confirm that the genetic ablation of β_1-integrin in β tumor cells results in specific deficiencies in their matrix adhesion and that NCAM signaling is epistatic to β_1-integrin-mediated cell–matrix adhesion in β tumor cells.

β_1-integrin but not NCAM is necessary for metastasis formation

We next asked whether cell lines deficient in either β_1-integrin or NCAM expression were able to form tumors and metastases in syngeneic tumor transplantation experiments *in vivo*. Equal numbers of $\beta Ti^{(fl/fl)}$, $\beta Ti^{(\Delta/\Delta)}$, βTN2 and βT2 cells were injected subcutaneously into the flanks of immunocompetent C57Bl/6 mice. After 5 weeks, mice were killed and tumor incidence, tumor size and tumor volumes were determined (Figure 4A and B). Primary tumors formed in 12.5% of all βT2-injected sites and in 37.5% of all $\beta Ti^{(fl/fl)}$-injected sites (Figure 4B). The average size of tumors from βT2 cells was $293.4 \pm 129.4\,mm^3$ as compared with $174.7 \pm 53.1\,mm^3$ for tumors arising from $\beta Ti^{(fl/fl)}$ cells (Figure 4A). In contrast, β_1-integrin-deficient $\beta Ti^{(\Delta/\Delta)}$ and NCAM-deficient βTN2 cells did not give rise to any tumors.

To assess the metastatic potential of these cell lines, we injected equal numbers of cells into the tail vein of athymic nu/nu mice. After 4 weeks, mice were killed, pancreata, lungs and livers of all mice were isolated, and subjected to histological and microscopic examination for metastatic lesions. All β tumor cell lines, with the exception of $\beta Ti^{(\Delta/\Delta)}$, lacking β_1-integrin expression, induced the formation of metastatic nodules in lungs and/or liver (Table II).

These results indicate that depletion of NCAM and therefore reduction of β_1-integrin activity in βTN2 cells diminishes tumor formation but still allows them to colonize distant organs. However, the total loss of β_1-integrin function results in an incapability to form primary tumors and colonizing nodules/metastases, indicating a critical role for β_1-integrin in these processes.

Reduced tumor cell proliferation in the absence of β_1-integrin

We next examined the effects of β_1-integrin depletion on RipTag2 tumorigenesis. Control and experimental mice were

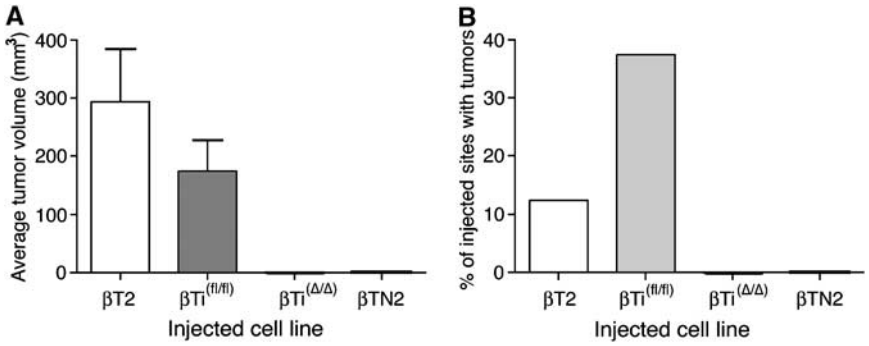

Figure 4 β_1-integrin-deficient β tumor cells do not form primary tumors or colonize distant organs in transplantation experiments. (**A**) Average volumes of tumors arising from transplanted β tumor cell lines. A total of 10^6 each of wild-type β tumor cells (βT2), cells carrying floxed alleles of the β_1-integrin gene ($\beta Ti^{(fl/fl)}$), cells deficient for β_1-integrin expression ($\beta Ti^{(\Delta/\Delta)}$) and cells deficient for NCAM expression (βTN2) were injected into the flanks of C57Bl/6 mice. (**B**) Tumor incidence in C57Bl/6 mice injected with the cell lines described in (A). Sixteen sites in eight mice were injected per genotype cell line, and the percentage of sites with tumors is presented.

Table II β_1-integrin-deleted cells are not able to metastasize[a]

Cell line	Number of injected mice	Number of mice with metastases	Site of metastasis
βT2	5	4	Lung/liver
$\beta Ti^{(fl/fl)}$	5	3	Lung
βTN2	5	4	Lung/liver
$\beta Ti^{(\Delta/\Delta)}$	5	0	—

[a]The different genotype β cell lines were injected into the tail vein of athymic nu/nu mice and colonization and metastatic outgrowth in distant organs was scored.

killed at the age of 12 weeks, shortly before the mice succumb to hypoglycemia caused by the insulin-expressing tumors. Tumor-bearing pancreata were excised and tumor incidence was scored by counting and measuring macroscopically visible (>1 mm) tumors. Tumor incidence (i.e. number of tumors per mouse; Figure 5A) remained unchanged in RCre;RT2;$\beta 1^{(fl/fl)}$ mice as compared with RT2;$\beta 1^{(fl/fl)}$ control mice. However, total tumor volumes per mouse were found to be significantly reduced by the absence of β_1-integrin in tumors of RCre;RT2;$\beta 1^{(fl/fl)}$ mice (Figure 5B).

We investigated whether the decreased tumor burden was due to reduced proliferation rates or increased apoptosis of tumor cells in β_1-integrin-deficient tumors. Mice were injected with BrdU before being killed, and tumor cell proliferation was determined by visualizing BrdU incorporation in histological sections, with antibodies against BrdU (Figure 5C). Tumor cell proliferation was significantly reduced in the absence of β_1-integrin in RCre;RT2;$\beta 1^{(fl/fl)}$ tumors as compared with tumors of RT2;$\beta 1^{(fl/fl)}$ mice. The apoptotic rate of β tumor cells, as determined by TUNEL staining of histological sections, was also reduced in tumors of RCre;RT2;$\beta 1^{(fl/fl)}$ mice as compared with tumors of RT2;$\beta 1^{(fl/fl)}$ mice (Figure 5D). Tumor progression, that is, the incidence of malignant cancer and metastasis, was not affected at all, since tumors of both genotypes showed a similar incidence of adenomas and grade 1, 2 and 3 carcinomas and no apparent metastasis (Figure 5E). It should be also noted that interfering with β_1-integrin function did not affect the onset, extent or quality of tumor angiogenesis, as assessed by staining for the endothelial cell marker CD31 (see above; Supplementary Figure 2).

Consistent with the *in vivo* observation described above, the growth rates of the β_1-integrin-deleted cell line $\beta Ti^{(\Delta/\Delta)}$ were significantly slower than that of the control cell line $\beta Ti^{(fl/fl)}$ (Figure 5F, $k=0.0014$ for $\beta Ti^{(\Delta/\Delta)}$ versus $k=0.0025$ for $\beta Ti^{(fl/fl)}$; $P<0.0001$, unpaired *t*-test of linear regression curves). The lack of β_1-integrin also affected the growth behavior of β tumor cells in a three-dimensional (3D) Matrigel™ culture system. Most of the cell spheres formed by $\beta Ti^{(fl/fl)}$ cells formed filopodia-like protrusions (Figure 6A, left panels), whereas $\beta Ti^{(\Delta/\Delta)}$ cells were unable to form these protrusions (Figure 6A, right panels). Quantification of this effect by counting cells with or without protrusion in a defined volume revealed that more than 70% of the $\beta Ti^{(fl/fl)}$ cells developed protrusions, whereas not a single of the β_1-integrin-deficient cells showed the formation of these structures. A week after plating, all $\beta Ti^{(\Delta/\Delta)}$ had died, whereas β_1-integrin-expressing $\beta Ti^{(fl/fl)}$ cells were still alive (data not shown).

Loss of β_1-integrin induces senescence in β cell tumors

The diminished levels of tumor cell proliferation as well as tumor cell apoptosis raises the possibility that β_1-integrin-deficient tumor cells might be impeded in entering and progressing through the cell cycle. To investigate the cell cycle status of cells from RT2;$\beta 1^{(fl/fl)}$ control tumors compared with RCre;RT2;$\beta 1^{(fl/fl)}$ experimental tumors, tumor cell suspensions of tumors from 12-week-old mice were stained with Pyronin Y (staining for RNA) and Hoechst 33342 (staining for DNA), allowing discrimination of cells in cell cycle phase G0, G1 or G2/S/M (Shapiro, 1981). Significantly more cells ($P<0.05$, unpaired *t*-test) derived from RCre; RT2;$\beta 1^{(fl/fl)}$ tumors were found to stall in G0 as compared with β_1-integrin-expressing control tumor cells (Figure 7A). Consistent with this observation, cultured β_1-integrin-deficient β tumor cells ($\beta Ti^{(\Delta/\Delta)}$) also exhibited a significantly increased cell cycle arrest in G0/G1 (Supplementary Figure 1).

Reduced metabolic activity and cell cycle arrest in G0 are associated with cellular quiescence, senescence and/or tumor dormancy. Senescence-associated β-galactosidase (SA-β-Gal) is expressed in senescent cells and is therefore frequently used as a marker for cellular senescence. It can be specifically detected at pH 6 by histochemical staining (Dimri *et al*, 1995). In contrast, bacterial β-galactosidase is most active at a pH of

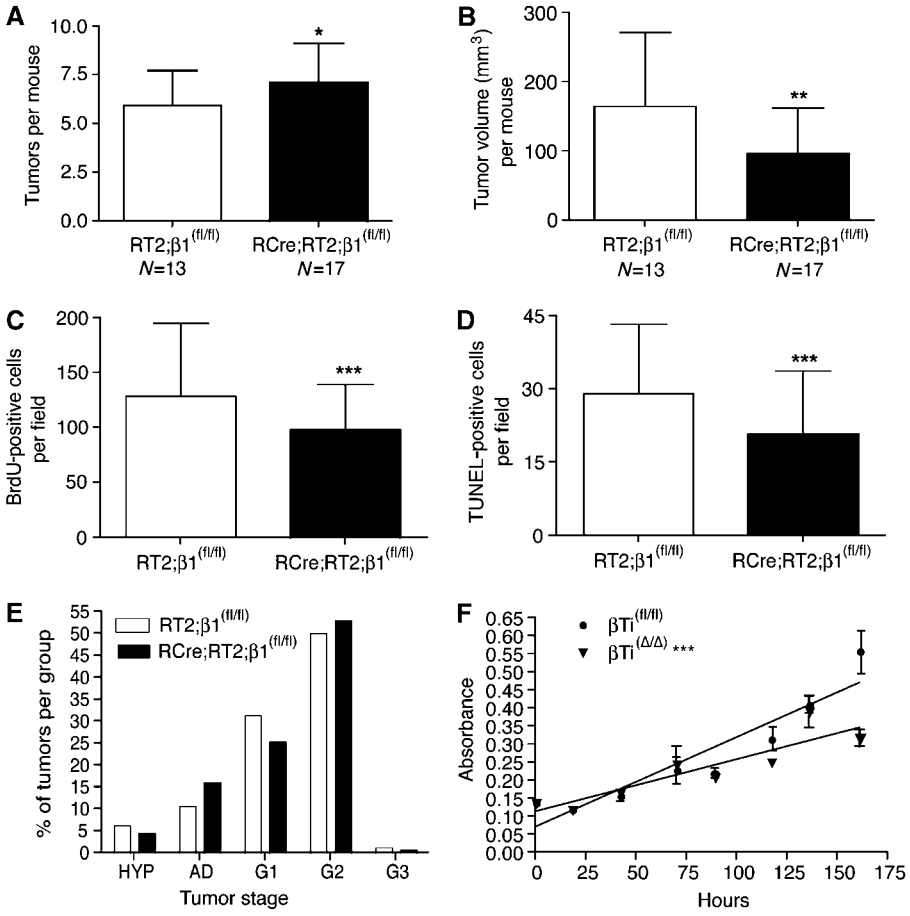

Figure 5 Reduced tumor cell proliferation and apoptosis in β_1-integrin-deficient RT2 tumors. Tumor incidences (**A**) and tumor volumes (**B**) of pancreata derived from RT2;$\beta1^{(fl/fl)}$ control and RCre;RT2;$\beta1^{(fl/fl)}$ mice. Tumor cell proliferation was visualized by BrdU staining (**C**) and apoptotic cells were visualized by TUNEL reaction (**D**). BrdU- or TUNEL-positive cells were counted per $\times 40$ microscopic field. $^*P>0.1$; $^{**}P<0.05$; $^{***}P<0.01$, unpaired *t*-test; *n*, number of analyzed mice. (**E**) Tumors of hematoxylin and eosin-stained sections were classified according to their histological grading. HYP, hyperplastic islets; AD, adenoma; G1, carcinoma grade1; G2, carcinoma grade 2; G3, carcinoma grade 3. (**F**) MTT growth assay of $\beta Ti^{(fl/fl)}$ and $\beta Ti^{(\Delta/\Delta)}$ tumor cell lines. Linear regression curves were calculated and are displayed for each cell line. $^*P<0.001$, unpaired *t*-test of linear regression curves.

7.5. Since the $\beta1^{(fl/fl)}$ mouse line used for the experiments described above has been generated in a way that, upon efficient recombination, a bacterial β-galactosidase reporter comes under the control of the β_1-integrin promoter, and because bacterial β-galactosidase also displays activity at pH 6, we could not test for SA-β-Gal in these mice. Therefore, we took advantage of an alternative mouse line in which the conditional β_1-integrin alleles do not carry a β-galactosidase reporter gene (β1EII mice). β1EII mice were intercrossed to the RT2 tumor model, giving rise to RCre;RT2;β1EII experimental and RT2;β1EII control mice. When compared to RCre;RT2;$\beta1^{(fl/fl)}$ mice, RCre;RT2;β1EII experimental mice exhibited an identical tumor phenotype, including a reduced tumor burden and increased tumor cell embolization in the lymphatics (data not shown). Notably, histological sections of tumors from RCre;RT2;β1EII showed positive staining for SA-β-Gal (Figure 7B, left and middle panels), whereas no staining was detectable in RT2;β1EII control mice (Figure 7B, right panels). A total of 57 control and 62 experimental tumors were investigated. Whereas the vast majority of control tumors did not stain for SA-β-Gal (Figure 7C, 98.2%), SA-β-Gal activity was detected in approximately 50% of experimental tumors (Figure 7C). Cultured β_1-integrin-deficient β tumor cells ($\beta Ti^{(\Delta/\Delta)}$) also exhibited increased activity of SA-β-Gal, as compared with the control cell line $\beta Ti^{(fl/fl)}$ (data not shown). These results suggest that deletion of β_1-integrin in RT2 tumors reduces tumor burden by inducing tumor cell senescence.

The cyclin-dependent kinase (CDK) inhibitor $p21^{Cip1}$ has been shown to be upregulated in various cell lines during senescence (Xiong *et al*, 1993; Alcorta *et al*, 1996), and increased expression of $p21^{Cip1}$ leads to the induction of a permanent growth arrest with characteristics of cellular senescence in several cancer cell types (Fang *et al*, 1999). Recent studies on alveolar epithelial cells correlated β_1-integrin-deficiency with inhibited luminal cell proliferation and a concomitant increase of $p21^{Cip1}$ expression (Li *et al*, 2005). We therefore investigated $p21^{Cip1}$ expression levels in tumor lysates derived from control (RT2;β1EII and RT2;$\beta1^{(fl/fl)}$) and β_1-integrin-deficient experimental (RCre;RT2;β1EII and RCre;RT2;$\beta1^{(fl/fl)}$) mice by quantitative immunoblotting (Figure 8A). Comparison of the relative $p21^{Cip1}$ protein levels revealed an increase of $p21^{Cip1}$ expression at an average of 7.7-fold in experimental tumors *in vivo* (Figure 8B). Upregulated expression of $p21^{Cip1}$ was also observed in $\beta Ti^{(\Delta/\Delta)}$ cells (Supplementary Figure 1B). No change in the expression of

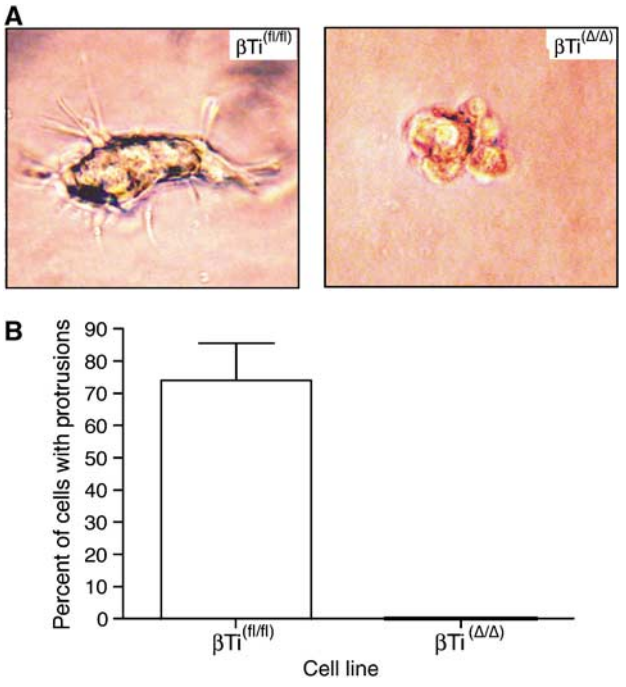

Figure 6 Impaired growth and filopodia formation of β_1-integrin-deficient β tumor cells in a 3D culture system. (**A**) Phase-contrast micrographs of control ($\beta Ti^{(fl/fl)}$) and β_1-integrin-deficient $\beta Ti^{(\Delta/\Delta)}$ β tumor cells 2 days after seeding in Matrigel™. (**B**) Quantification of protrusion formation of $\beta Ti^{(fl/fl)}$ and $\beta Ti^{(\Delta/\Delta)}$ cells grown as in (A).

any other cell cycle inhibitors or cell cycle regulatory genes tested (p15, p16, p27, p57, cyclin D2, cyclin E) was observed; only the expression of cyclin B was moderately increased in the absence of β_1-integrin function. This suggests that loss of β_1-integrin in β tumor cells induces cellular senescence by a pathway that involves, among other molecular processes, upregulated expression of the CDK inhibitor $p21^{Cip1}$.

Discussion

Recent work from several laboratories, including our own, has demonstrated that the loss of NCAM function during β cell carcinogenesis in RT2 transgenic mice results in the loss of β_1-integrin activation, tumor tissue disintegration, upregulated lymphangiogenesis and, finally, in metastasis to regional lymph nodes (Perl *et al*, 1999; Cavallaro *et al*, 2001; Crnic *et al*, 2004; Xian *et al*, 2006). Motivated by these observations, we set out to assess whether the loss of β_1-integrin had any impact on RT2 tumorigenesis and whether it phenocopied the loss of NCAM function. Specific inactivation of β_1-integrin by Cre-mediated recombination of loxP-flanked β_1-integrin alleles occurred in approximately 40% of tumor cells and resulted in the dissemination of tumor cell emboli into the lymphatic vasculature, yet did not induce lymphangiogenesis. Notably, β_1-integrin-deficient tumor cells displayed decreased rates of proliferation and apoptosis by acquiring cellular senescence. Moreover, β tumor cell lines lacking β_1-integrin expression were unable to form tumors or to colonize distant organs in tumor transplantation experiments. Together, the results indicate that β_1-integrin plays a critical role in tumor outgrowth by preventing cellular senescence, the lymphogenic dissemination of tumor cell emboli and their colonization of distant metastatic sites.

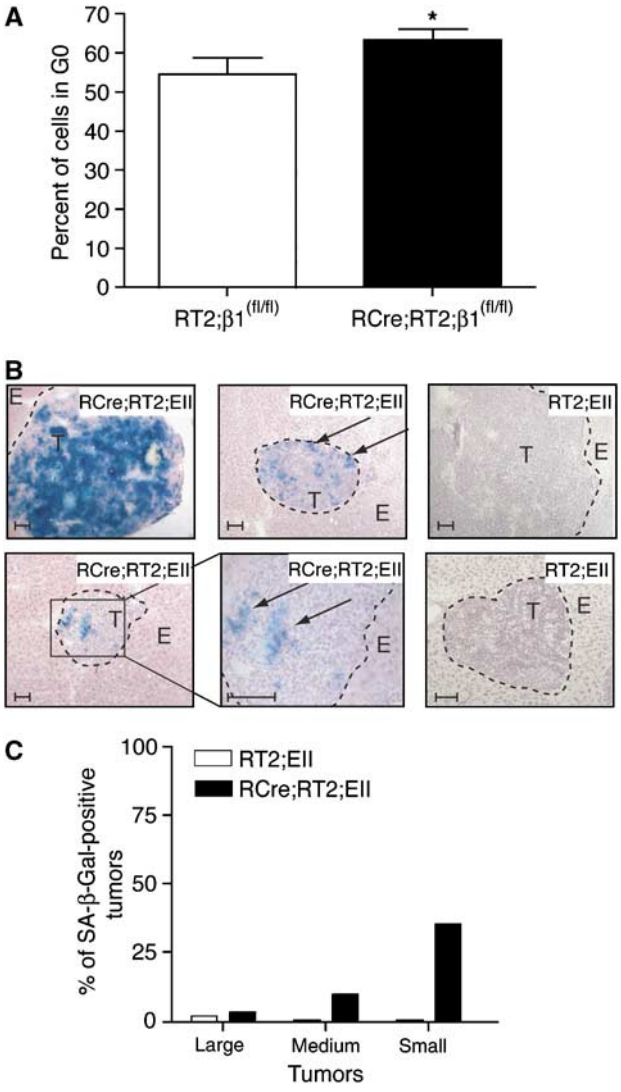

Figure 7 The lack of β_1-integrin function induces cellular senescence. (**A**) Cell cycle analysis of tumors derived from $RT2;\beta1^{(fl/fl)}$ and $RCre;RT2;\beta1^{(fl/fl)}$ mice, as indicated. Three animals were analyzed per genotype. The percentages of cells in G0 are plotted. $^*P<0.05$, unpaired *t*-test. (**B**) Examples of tumor cells of RCre;RT2;EII mice exhibiting expression of SA-β-Gal (turquoise, left and middle panels). Control tumors (RT2;EII, expressing β_1-integrin) do not show any detectable signal for SA-β-Gal (right panels). Scale bar, 50 μm. T, tumor; E, exocrine pancreas; (**C**) Percentages of SA-β-Gal-positive and SA-β-Gal-negative tumors of RT2;EII (white bars) and RCre;RT2;EII (black bars) mice. Large, medium and small refer to tumor sizes of >3 mm, >1 mm and <1 mm in diameter, respectively.

Defects in endocrine cell sorting during islet development

Besides mild defects in the development of the nervous system, the loss of NCAM function in $NCAM^{-/-}$ mice results in a cell sorting defect during the development of the islets of Langerhans (Esni *et al*, 1999). In normal islets of Langerhans, glucagon-producing α cells are located at the periphery of the islets, whereas insulin-producing β cells localize to the center of the islets. In the absence of NCAM expression, α and β cells are intermixed in the islets. Here, we report an identical phenotype in $RCre;\beta1^{(fl/fl)}$ mice, in which β_1-integrin function is specifically ablated in β cells during islet development. Also here, the intermixing of α and β cells does not affect islet

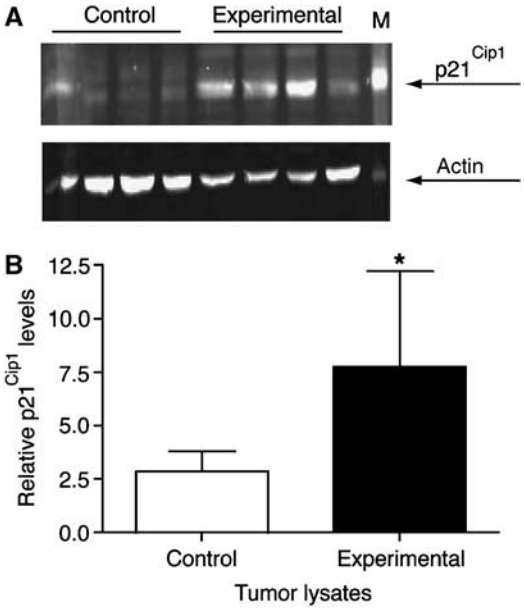

Figure 8 Increased $p21^{Cip1}$ levels in β_1-integrin-deficient tumors. (**A**) Immunoblot for actin and $p21^{Cip1}$ levels in lysates from control ($RT2;\beta1^{(fl/fl)}$ and RT2;EII) and β_1-integrin-deficient (RCre;RT2;$\beta1^{(fl/fl)}$ and RCre;RT2;EII) tumors. M, molecular weight marker. (**B**) Quantification of relative $p21^{Cip1}$ levels as determined by fluorescent quantitative immunoblotting shown in (A). $^*P<0.05$, unpaired *t*-test.

physiology or metabolism of the animal. These results indicate that the loss of β_1-integrin recapitulates the loss of NCAM in islet development, further supporting the epistatic link between NCAM and β_1-integrin functions.

Tumor cell emboli but no metastasis

Increased tumor lymphangiogenesis has been demonstrated to correlate with the incidence of lymph node metastasis in many experimental systems and cancer types in patients (Cao, 2005). Interestingly, in tumors of NCAM-deficient RT2 mice, the expression of the two lymphangiogenic factors VEGF-C and D was found to be upregulated, and interference with their activities resulted in a repression of lymphangiogenesis and lymph node metastasis in these mice (Crnic *et al*, 2004). $RT2;NCAM^{-/-}$ tumors also show severe tissue disintegration and the appearance of large hemorrhagic lacunae. A recent report linked increased blood hemorrhage and the concomitant tissue disintegration phenotype to decreased pericyte recruitment to endothelial cells (Xian *et al*, 2006). Notably, interference with pericyte recruitment by ablating PDGF B function during β cell carcinogenesis in RT2 mice resulted in blood vessel hemorrhage and tumor metastasis in the absence of lymphangiogenesis (Xian *et al*, 2006). However, since the observed tissue disintegration of NCAM-deficient β cell tumors may potentially also result from a loss of β_1-integrin-mediated cell adhesion (Cavallaro *et al*, 2001), we assessed whether the inactivation of β_1-integrin might be responsible for the upregulated lymphangiogenesis observed in $RT2;NCAM^{-/-}$ mice. Our results show that β_1-integrin deletion does not lead to an upregulated expression of the lymphangiogenic factors VEGF-C or VEGF-D and to tumor lymphangiogenesis and, thus, that the increased lymphangiogenesis observed in $RT2;NCAM^{-/-}$ mice is not directly due to a defect in β_1-integrin function.

In $RCre;RT2;\beta1^{(fl/fl)}$ mice, tumor architecture *per se* is not altered, but clusters of tumor cell emboli are found circulating in lymphatic vessels in the absence of activated lymphangiogenesis. Disseminated tumor cell emboli are also found in $RT2;NCAM^{-/-}$ mice, although in the presence of lymphangiogenesis, suggesting that in NCAM-deficient tumors two different mechanisms are employed: impaired pericyte recruitment (Xian *et al*, 2006) and loss of cell matrix adhesion (this work). Both of these processes result in tumor cell dissemination and lymph node metastasis.

Taken together, the results reported here support our previous findings that the loss of β_1-integrin function in β cells reduces their cell–matrix adhesion and causes tumor cell dissemination. However, the results indicate that the loss of β_1-integrin function by itself does not lead to an induction of tumor lymphangiogenesis and to lymph node metastasis.

β_1-integrin signaling is required for metastasis formation

We have employed a variety of β tumor cell lines established from RT2 tumors in adhesion, proliferation and transplantation assays, to discriminate the role of adhesive and growth promoting integrin functions (Table III). Control βT2 cells have very high NCAM levels and hence show high levels of β_1-integrin activation. βTN2 cells lack NCAM expression and thus NCAM-dependent, β_1-integrin-mediated matrix adhesion. In contrast, β tumor cell lines established from $RCre;RT2;\beta1^{(fl/fl)}$ tumors ($\beta Ti^{(\Delta/\Delta)}$ cells) lack β_1-integrin expression.

In contrast to the tumor cell emboli in $RT2;NCAM^{-/-}$ mice, which disseminate to local lymph nodes, tumor cell emboli in $RCre;RT2;\beta1^{(fl/fl)}$ mice are not able to form metastasis. Consistent with this notion, $\beta Ti^{(\Delta/\Delta)}$ cells that lack β_1-integrin expression also do not grow primary tumors or colonize distant organs when injected into the tail veins of immunodeficient mice. This failure may not be due to their loss of β_1-integrin-mediated cell–matrix adhesion, since βTN2 cells, which lack NCAM-dependent activation of β_1-integrin and thus cell adhesion, can still metastasize. On the other hand, both cell lines fail to form primary tumors when injected under the skin, suggesting that both NCAM and β_1-integrin are required for primary tumor growth. These results are consistent with published work reporting that β_1-integrin-deficient ES cells fail to efficiently form teratomas in transplanted mice (Bloch *et al*, 1997).

Together, the data indicate that β_1-integrin is required to allow cells to survive and proliferate at distant sites. This notion is consistent with a previous report that unligated integrins induce caspase 8-dependent integrin-mediated cell death (IMD; Stupack *et al*, 2001). However, β_1-integrin is required for establishing primary tumors in transplantation experiments, yet not in endogenously growing tumors of RT2 transgenic mice. This difference is likely due to the specific tumor microenvironment that may compensate for the loss of β_1-integrin function.

Loss of β_1-integrin induces cellular senescence

In β_1-integrin-deficient tumors of $RCre;RT2;\beta1^{(fl/fl)}$ mice, tumor volumes, but not tumor incidence and tumor progression, is reduced as compared with control mice. Lack of

Table III Characterization of β tumor cell lines

Cell line	NCAM expr.[a]	Col IV adhesion[b]	2D[c]	3D[d]	s.c.[e]	i.v.[f]
βT2	+ + +	+	+	+[g]	+	+
$\beta Ti^{(fl/fl)}$	+	+	+	+	+	+
βTN2	−	+[h]	+	+[g]	−	+
$\beta Ti^{(\Delta/\Delta)}$	+	−	±	−	−	−

[a]NCAM expression levels of cell lines: + + +, high levels; +, low levels; −, no expression.
[b]Adhesion to collagen IV stimulatable by NCAM transfection: +, stimulatable; −, not stimulatable.
[c]Growth of cell lines in 2D cultures: +, fast growth; ±, slow growth.
[d]Growth of cell lines in Matrigel: +, growth; −, no growth.
[e]Tumor growth after subcutaneous injection: +, tumors growth; −, no tumor formation.
[f]Lung metastasis after intravenous injection: +, metastases; −, no metastases.
[g]Data not shown.
[h]Also shown in Cavallaro *et al* (2001).

cell–matrix adhesion may result in a loss of signals for cell survival and proliferation and the induction of anoikis, that is, apoptosis caused by the lack of cell attachment (Frisch and Ruoslahti, 1997). However, both the rate of tumor cell apoptosis and proliferation are found reduced in β_1-integrin-deficient RCre;RT2;$\beta1^{(fl/fl)}$ tumors as compared with β_1-integrin-expressing control tumors. A similar effect of β_1-integrin function has been previously reported in various models of breast carcinogenesis, where its loss also represses tumor cell proliferation in the absence of increased apoptosis (White *et al*, 2004; Li *et al*, 2005). In these experiments, the loss of β_1-integrin correlates with reduced phosphorylation of focal adhesion kinase (FAK), an increased expression of the cell cycle inhibitory protein $p21^{Cip1}$, and the arrest of cells in the G1 phase of the cell cycle. Consistent with these reports, we find that the expression of $p21^{Cip1}$ is also upregulated in tumors of RCre;RT2;$\beta1^{(fl/fl)}$ mice. Moreover, β_1-integrin-deficient β tumor cells are retained in the G0/G1 phase of the cell cycle and acquire the expression of SA-β-Gal, all specific marker for cellular senescence.

Together, the results in RT2 transgenic mice and β cell tumor cell lines derived thereof indicate that targeting β_1-integrin function induces cellular senescence and represses the metastatic potential of β tumor cell lines. Hence, interfering with the function of β_1-integrin during tumor progression, for example, by neutralizing antibodies or by antagonistic peptides, may offer a valid approach for cancer treatment. In fact, recent studies on mammary epithelial cell lines indicate that blocking β_1-integrin function inhibits proliferation and tumorigenic morphology of cultured breast cancer cells (Weaver *et al*, 1997; Wang *et al*, 2002). Our results now raise the intriguing possibility that the ablation of β_1-integrin function results in the induction of cellular senescence in tumor cells, a potential therapeutic goal. Future experimentation is warranted to elucidate the molecular players and pathways underlying the induction of cellular senescence upon loss of β_1-integrin function.

Materials and methods

Transgenic mice

Generation and phenotypic characterization of Rip1Tag2 mice, RCre mice and $\beta1^{(fl/ff)}$ mice have been described previously (Hanahan, 1985; Ahlgren *et al*, 1998; Potocnik *et al*, 2000). β1EII mice will be described elsewhere (R Fässler, unpublished results). All mouse lines were backcrossed to C57Bl/6 for at least five generations. All experiments involving mice were performed in accordance with the guidelines of the Swiss Federal Veterinary Office (SFVO) and the regulations of the Cantonal Veterinary Office of Basel-Stadt.

Histological analysis

All mice were killed between 12 and 13 weeks of age, unless otherwise stated. Tumor incidence per mouse was determined by counting all macroscopically apparent tumors with a minimal diameter of 1 mm. Tumor volume was defined as total tumor volume per mouse in mm^3, calculated by measuring the tumor diameters assuming a spherical shape of the tumors.

Tumors and pancreata were fixed overnight in 4% paraformaldehyde in PBS, dehydrated and paraffin embedded. Tissue sections (5 μm thick) were deparaffinized and rehydrated before histological and immunohistochemical stainings.

Tumors were categorized into subclasses by inspection of hematoxylin-/eosin-stained histological sections: normal/hyperplastic, adenoma, carcinoma grade 1 (well differentiated, one invasive tumor edge), carcinoma grade 2 (partially dedifferentiated, tumor capsule largely absent, more than one invasive tumor edge), carcinoma grade 3 or anaplastic tumor (complete loss of tumor cell differentiation).

The following antibodies were used for immunohistochemical or immunofluorescence stainings on paraffin sections: guinea pig anti-insulin (DakoCytomation, Glostrup, Denmark), rabbit anti-mouse LYVE-1 (Reliatech, Braunschweig, Germany), goat anti-glucagon (Santa Cruz, Santa Cruz, CA, USA), biotinylated mouse anti-BrdU (Zymed, South San Francisco, CA, USA), *In situ* Cell Death Detection kit, (TUNEL, Roche, Basel, Switzerland). All biotinylated secondary antibodies for immunohistochemistry (Vector, Burlingame, CA, USA) were used at a 1:200 dilution, and positive staining was visualized with the ABC horseradish peroxidase kit (Vector, Burlingame, CA, USA) and DAB Peroxidase Substrate (Sigma Chemical Co., St Louis, MO, USA), according to the manufacturers' recommendations. For the analysis of tissue morphology, slides were slightly counterstained with hematoxylin or eosin. Alexa Fluor 568- and 488-labeled secondary antibodies (Molecular Probes, Eugene, OR, USA) diluted 1:400 were used for immunofluorescence analysis. 6-Diamidino-2-phenylindole (DAPI, Sigma) was used for nuclear staining in immunofluorescence stainings. All paraffin-embedded sections were subject to antigen retrieval with 10 mM citrate buffer (microwave), except with stainings for insulin and glucagon (10 min in 0.2% Triton X-100 in PBS), BrdU (1 h in 2 N HCl and subsequently 1 h 1 × trypsin at room temperature (RT)) and TUNEL (10 min 2 μg/ml proteinase K (Sigma) at RT).

For BrdU labeling, 100 μg BrdU (Sigma) per gram body weight was injected 90 min before killing the mice. To determine tumor cell proliferation/apoptotic indices, BrdU/TUNEL-positive nuclei were counted per randomly chosen × 40 magnification field of tumor tissue. Approximately 10 fields per mouse were counted.

Lymphangiogenesis was quantified by assessing the extent by which LYVE-1-positive lymphatic vessels surrounded the tumor perimeter: tumors that were not in contact with any lymphatic vessel (0%), tumors that were surrounded less than 10% (<10%), less than 25% (<25%), less than 50% (<50%) and tumors that were surrounded by lymphatics more than 50% of the tumor perimeter (>50%).

For immunohistochemical detection of SA-β-Gal, 20 μm sections of frozen tissues were cut and fixed in 70% ethanol for 3 min and treated as described (Dimri *et al*, 1995).

Stained sections were viewed on an Axioskop 2 plus light microsope, using axiovision 3.1. software (Zeiss, Feldbach, Switzerland), or a Nikon Diaphot 300 immunofluorescence microscope (Nikon, Egg, Switzerland), using Openlab 3.1.7. software (Improvision, Coventry, England). Insulin and glucagon staining per islet area was determined from images of insulin- and glucagon-stained slides obtained using ImageJ software at the National Institutes of Health (http://rsb.info.nih.gov/ij/). All statistical analyses were performed using GraphPad software (GraphPad, San Diego, CA, USA).

Cell culture

All cell lines were grown in DMEM supplemented with 10% fetal bovine serum, 2 mmol/l glutamine and 100 U/ml penicillin. Tumor

cell lines were established from insulinomas of 12-week-old RT2;$\beta1^{(fl/fl)}$ and RCre;RT2;$\beta1^{(fl/fl)}$ mice, as described (Cavallaro *et al*, 2001). For transplantation of tumor cells, 10^6 cells in PBS were injected subcutaneously into the two flanks of C57Bl/6 mice, or intravenously into athymic nu/nu mice.

Matrix adhesion assays were performed on collagen IV, as described (Cavallaro *et al*, 2001). Ninety-six-well plates were coated with 5 μg/cm^2 of mouse collagen IV (BD Biosciences, San Jose, CA, USA). A total of 6×10^4 cells were seeded per well, and after 90 min non-adherent cells were removed by washing with PBS. Adherent cells were fixed for 20 min with 25% glutaraldehyde (Sigma), stained with crystal violet, washed and air-dried. Bound dye was solubilized with 10% acetic acid and absorbance measured at 595 nm. Cell-free wells served as blanks. The assays were performed in triplicates.

For proliferation assays, 10^5 cells were seeded per well of a 24-well plate. Every 24 h, 100 μl MTT (3-(4,5-dimethylthiazol-2-yl)-2,5-diphenyltetrazolium bromide (Sigma), 5 mg/ml in PBS) was added, and 90 min later medium was removed, 500 μl solubilization buffer (95% isopropanol, 5% formic acid) was added and incubated for 5 min at RT. Absorbance of the solution was determined at 570 nm.

For growth in 3D culture, 5×10^4 cells were mixed in Matrigel™ (BD Biosciences) and seeded on a layer of solidified Matrigel™. After solidification of the upper cell-containing Matrigel™ layer, normal growth medium was added to the culture.

FACS analysis of tumors

Tumors were dissected out of pancreata, placed in ice-cold PBS and minced into small pieces. After washing with PBS, tumor pieces were incubated, for 30 min at 37°C, with a collagenase mix DMEM, 5% NU-serum (BD Biosciences), 0.16 mg/ml DNase I, 1 mg/ml collagenase D, H and collagenase/dispase (Roche), 0.5 mg/ml collagenase I (Sigma), to obtain single-cell suspensions, followed by filtration and washing with FACS–PBS (1× PBS, 5% FCS). Tumor cell suspensions were incubated with anti-β1-integrin-FITC (Serotec, Oxford, UK) and anti-CD31-PE (PharMingen, Franklin Lakes, NJ, USA) antibodies and analyzed with a FacsScan (BD Biosciences, San Jose, CA, USA), using CellQuest software. For cell cycle analysis, tumor cell suspensions were incubated with Pyronin Y (Sigma) and Hoechst 33342 (Molecular Probes), as described in Shapiro (1981).

Immunoblotting

Lysates from cell lines were prepared as described (Cavallaro *et al*, 2001). Tumors were isolated and frozen in liquid N_2. Tumor lysis buffer (10 mM Tris pH 8, 100 mM NaCl, 2.5 mM EDTA, proteinase inhibitors (Crnic *et al*, 2004) and 0.5% Triton X-100) was added and tumors were homogenized. After centrifugation (4°C, 13 000 r.p.m., 30 min) supernatants were subjected to immunoblotting. Primary antibodies were: NCAM (NCAM13, PharMingen), actin (actin I-19, Santa Cruz) and $p21^{Cip1}$ (p21 H-164, Santa Cruz); secondary antibodies were: peroxidase-conjugated donkey anti-mouse IgG (Jackson ImmunoResearch, West Grove, PA, USA), biotinylated anti-goat IgG (Vector), goat anti-rabbit IRDye™680 (Li-Cor Biosciences, Lincoln, NE, USA) and IRDye™800CW streptavidin (Li-Cor Biosciences). Proteins were visualized using the Uptilight Chemiluminescence kit (Uptima, Interchim, Montiuçon, France) or the Odyssey Infrared Imaging System, and quantification of protein levels was performed using the Odyssey Software (Li-Cor Biosciences).

Supplementary data

Supplementary data are available at *The EMBO Journal* Online (http://www.embojournal.org).

Acknowledgements

We thank M Lewerenz for preliminary experiments, V Jäggin for help in the cell cycle analysis of tumors, and U Schmieder for mouse genotyping. This work was supported by the EU-FP6 framework programme LYMPHANGIOGENOMICS LSHG-CT-2004-503573 (GC), the NCCR Molecular Oncology of the Swiss National Science Foundation (GC), and the Agency for International Cancer Research (UC).

References

Ahlgren U, Jonsson J, Jonsson L, Simu K, Edlund H (1998) Beta-cell-specific inactivation of the mouse Ipf1/Pdx1 gene results in loss of the beta-cell phenotype and maturity onset diabetes. *Genes Dev* **12:** 1763–1768

Alcorta DA, Xiong Y, Phelps D, Hannon G, Beach D, Barrett JC (1996) Involvement of the cyclin-dependent kinase inhibitor p16 (INK4a) in replicative senescence of normal human fibroblasts. *Proc Natl Acad Sci USA* **93:** 13742–13747

Banerji S, Ni J, Wang SX, Clasper S, Su J, Tammi R, Jones M, Jackson DG (1999) LYVE-1, a new homologue of the CD44 glycoprotein, is a lymph-specific receptor for hyaluronan. *J Cell Biol* **144:** 789–801

Bloch W, Forsberg E, Lentini S, Brakebusch C, Martin K, Krell HW, Weidle UH, Addicke K, Fassler R (1997) Beta 1 integrin is essential for teratoma growth and angiogenesis. *J Cell Biol* **139:** 265–278

Brooks PC, Clark RA, Cheresh DA (1994) Requirement of vascular integrin alpha v beta 3 for angiogenesis. *Science* **264:** 569–571

Brooks PC, Stromblad S, Klemke R, Visscher D, Sarkar FH, Cheresh DA (1995) Anti-integrin alpha v beta 3 blocks human breast cancer growth and angiogenesis in human skin. *J Clin Invest* **96:** 1815–1822

Cao Y (2005) Opinion: emerging mechanisms of tumour lymphangiogenesis and lymphatic metastasis. *Nat Rev Cancer* **5:** 735–743

Cavallaro U, Niedermeyer J, Fuxa M, Christofori G (2001) N-CAM modulates tumour-cell adhesion to matrix by inducing FGF-receptor signalling. *Nat Cell Biol* **3:** 650–657

Crnic I, Strittmatter K, Cavallaro U, Kopfstein L, Jussila L, Alitalo K, Christofori G (2004) Loss of neural cell adhesion molecule induces tumor metastasis by upregulating lymphangiogenesis. *Cancer Res* **64:** 8630–8638

Dahl U, Sjodin A, Semb H (1996) Cadherins regulate aggregation of pancreatic beta-cells *in vivo*. *Development* **122:** 2895–2902

Dimri GP, Lee X, Basil G, Acosta M, Scott G, Roskelley C, Medrano EE, Linskens M, Rubelj I, Pereira-Smith O, Peacocke M, Campisi J (1995) A biomarker that identifies senescent human cells in culture and in aging skin *in vivo*. *Proc Natl Acad Sci USA* **92:** 9363–9367

Esni F, Taljedal IB, Perl AK, Cremer H, Christofori G, Semb H (1999) Neural cell adhesion molecule (N-CAM) is required for cell type segregation and normal ultrastructure in pancreatic islets. *J Cell Biol* **144:** 325–337

Fang L, Igarashi M, Leung J, Sugrue MM, Lee SW, Aaronson SA (1999) p21Waf1/Cip1/Sdi1 induces permanent growth arrest with markers of replicative senescence in human tumor cells lacking functional p53. *Oncogene* **18:** 2789–2797

Fassler R, Meyer M (1995) Consequences of lack of beta 1 integrin gene expression in mice. *Genes Dev* **9:** 1896–1908

Friedlander M, Brooks PC, Shaffer RW, Kincaid CM, Varner JA, Cheresh DA (1995) Definition of two angiogenic pathways by distinct alpha v integrins. *Science* **270:** 1500–1502

Frisch SM, Ruoslahti E (1997) Integrins and anoikis. *Curr Opin Cell Biol* **9:** 701–706

Fujita Y, Krause G, Scheffner M, Zechner D, Leddy HE, Behrens J, Sommer T, Birchmeier W (2002) Hakai, a c-Cbl-like protein, ubiquitinates and induces endocytosis of the E-cadherin complex. *Nat Cell Biol* **4:** 222–231

Guo W, Giancotti FG (2004) Integrin signalling during tumour progression. *Nat Rev Mol Cell Biol* **5:** 816–826

Guo W, Pylayeva Y, Pepe A, Yoshioka T, Muller WJ, Inghirami G, Giancotti FG (2006) Beta 4 integrin amplifies ErbB2 signaling to promote mammary tumorigenesis. *Cell* **126:** 489–502

Hanahan D (1985) Heritable formation of pancreatic beta-cell tumours in transgenic mice expressing recombinant insulin/simian virus 40 oncogenes. *Nature* **315:** 115–122

Hynes RO (2002) Integrins: bidirectional, allosteric signaling machines. *Cell* **110:** 673–687

Li N, Zhang Y, Naylor MJ, Schatzmann F, Maurer F, Wintermantel T, Schuetz G, Mueller U, Streuli CH, Hynes NE (2005) Beta1 integrins regulate mammary gland proliferation and maintain the integrity of mammary alveoli. *EMBO J* **24:** 1942–1953

Naylor MJ, Li N, Cheung J, Lowe ET, Lambert E, Marlow R, Wang P, Schatzmann F, Wintermantel T, Schuetz G, Clarke AR, Mueller U, Hynes NE, Streuli CH (2005) Ablation of beta1 integrin in mammary epithelium reveals a key role for integrin in glandular morphogenesis and differentiation. *J Cell Biol* **171:** 717–728

Novak A, Hsu SC, Leung-Hagesteijn C, Radeva G, Papkoff J, Montesano R, Roskelley C, Grosschedl R, Dedhar S (1998) Cell adhesion and the integrin-linked kinase regulate the LEF-1 and beta-catenin signaling pathways. *Proc Natl Acad Sci USA* **95:** 4374–4379

Perl AK, Dahl U, Wilgenbus P, Cremer H, Semb H, Christofori G (1999) Reduced expression of neural cell adhesion molecule induces metastatic dissemination of pancreatic beta tumor cells. *Nat Med* **5:** 286–291

Potocnik AJ, Brakebusch C, Fassler R (2000) Fetal and adult hematopoietic stem cells require beta1 integrin function for colonizing fetal liver, spleen, and bone marrow. *Immunity* **12:** 653–663

Shapiro HM (1981) Flow cytometric estimation of DNA and RNA content in intact cells stained with Hoechst 33342 and pyronin Y. *Cytometry* **2:** 143–150

Stupack DG, Puente XS, Boutsaboualoy S, Storgard CM, Cheresh DA (2001) Apoptosis of adherent cells by recruitment of caspase-8 to unligated integrins. *J Cell Biol* **155:** 459–470

Sudhakar A, Sugimoto H, Yang C, Lively J, Zeisberg M, Kalluri R (2003) Human tumstatin and human endostatin exhibit distinct antiangiogenic activities mediated by alpha v beta 3 and alpha 5 beta 1 integrins. *Proc Natl Acad Sci USA* **100:** 4766–4771

Tan C, Costello P, Sanghera J, Dominguez D, Baulida J, de Herreros AG, Dedhar S (2001) Inhibition of integrin linked kinase (ILK) suppresses beta-catenin-Lef/Tcf-dependent transcription and expression of the E-cadherin repressor, snail, in APC−/− human colon carcinoma cells. *Oncogene* **20:** 133–140

Wang F, Hansen RK, Radisky D, Yoneda T, Barcellos-Hoff MH, Petersen OW, Turley EA, Bissell MJ (2002) Phenotypic reversion or death of cancer cells by altering signaling pathways in three-dimensional contexts. *J Natl Cancer Inst* **94:** 1494–1503

Weaver VM, Petersen OW, Wang F, Larabell CA, Briand P, Damsky C, Bissell MJ (1997) Reversion of the malignant phenotype of human breast cells in three-dimensional culture and *in vivo* by integrin blocking antibodies. *J Cell Biol* **137:** 231–245

White DE, Kurpios NA, Zuo D, Hassell JA, Blaess S, Mueller U, Muller WJ (2004) Targeted disruption of beta1-integrin in a transgenic mouse model of human breast cancer reveals an essential role in mammary tumor induction. *Cancer Cell* **6:** 159–170

Xian X, Hakansson J, Stahlberg A, Lindblom P, Betsholtz C, Gerhardt H, Semb H (2006) Pericytes limit tumor cell metastasis. *J Clin Invest* **116:** 642–651

Xiong Y, Hannon GJ, Zhang H, Casso D, Kobayashi R, Beach D (1993) p21 is a universal inhibitor of cyclin kinases. *Nature* **366:** 701–704

Zamir E, Geiger B (2001) Molecular complexity and dynamics of cell–matrix adhesions. *J Cell Sci* **114:** 3583–3590

Zhang F, Tom CC, Kugler MC, Ching TT, Kreidberg JA, Wei Y, Chapman HA (2003) Distinct ligand binding sites in integrin alpha3beta1 regulate matrix adhesion and cell–cell contact. *J Cell Biol* **163:** 177–188

